

Effect of Chronic Unpredictable Mild Stress on Adrenal Cortex of Adult Rat and The Possible Protective Role of Licorice Extract: A Histological and Immunohistochemical Study

Mona T. Sadek, Shereen S. El-Abd and Marwa A. A. Ibrahim

Histology and Cell Biology Department, Faculty of Medicine, Tanta University, Egypt

ABSTRACT

Background: Chronic stress, evolving due to sudden unexpected life events, is a risk factor for the development of depression. It can suppress immunity and increase susceptibility to inflammatory diseases. Licorice extract is commonly used in traditional and modern medicine particularly for its antioxidant and anti-inflammatory properties.

Aim of the Work: This work aimed to perform a biochemical, histological, and immunohistochemical assessment of the influence of chronic unpredictable mild stress (CUMS) on the structure of the adrenal cortex of rat and the possible ameliorating role of licorice aqueous extract.

Material and Methods: Twenty-four adult male albino rats were divided into 4 groups; control, licorice, CUMS (exposed to variable stressors in a random unpredictable pattern for 4 weeks), and licorice & CUMS (same as group III along with 300 mg/kg/day of licorice extract). Plasma aldosterone and corticosterone were assayed. Adrenal cortex specimens were processed for biochemical, histological, and immunohistochemical studies.

Results: CUMS group recorded a significant elevation of plasma aldosterone, corticosterone, tissue malondialdehyde and myeloperoxidase associating with a significant reduction of tissue reduced glutathione and superoxide dismutase. Histological examination revealed adrenal capsular thickening and subcapsular hyperplasia, disruption of the architecture and thickness of all zones, and cellular alterations as nuclear abnormalities and cytoplasmic vacuolation. A significant upregulation in both activated caspase-3 and PCNA immunohistochemical expression was recorded. Licorice co-treated group depicted near normal values of most parameters with a near control morphology.

Conclusion: Licorice could prove beneficial in controlling the adverse effects exerted by CUMS on redox status, morphology, apoptosis, and proliferation of the adrenal cortex most probably through its antioxidant, anti-inflammatory, and antiproliferative properties.

Received: 11 October 2020, **Accepted:** 05 November 2020

Key Words: Adrenal cortex; caspase-3; licorice; PCNA; stress.

Corresponding Author: Marwa A. A. Ibrahim, MD, Histology Department, Faculty of Medicine, Tanta University, 31527 Tanta, Egypt, **Tel.:** +201 0991 86399, **E-mail:** marwa.ibrahim@med.tanta.edu.eg; maleox68@yahoo.com

ISSN: 1110-0559, Vol. 44, No.4

INTRODUCTION

Humans are liable to variable stressful unexpected life events, e.g. COVID-19 pandemic, or even suffer internal stress as chronic inflammation.^[1,2] Chronic stress heightens the risk of incidence of sleep disorders, anxiety and depression.^[2,3] Depression affects the life quality in about 20% of the world's general population and was suggested to become one of the top reasons for global disability by 2020 according to the world health organization.^[4,5] Chronic stress was reported to suppress immunity and increase susceptibility to inflammatory diseases.^[1]

Chronic unpredictable mild stress paradigm (CUMS) is a well-known model established in rodents to simulate minor unanticipated everyday stressful life events to which humans are exposed.^[6] The stressors used in this paradigm are well-known to induce behavioral reactions to anxiety and fear in the rodents. Those stressors are employed unpredictably to prevent habituation. They are applied over a long period to induce anhedonia, which is a state of

decreased interest and pleasure that represents a common feature of depression.^[7]

During stress, both hypothalamic-pituitary-adrenocortical and sympatho-adrenomedullary axes are concerned with the maintenance of homeostasis. The adrenal gland is a common organ of both axes that plays an essential role in response to stress.^[8] Functionally, the adrenal gland is formed of two different organs; the cortex and the medulla. The adrenal cortex is concerned with the secretion of steroid hormones that mediate body homeostasis and response to chronic stress. Whereas the adrenal medulla synthesizes and secretes catecholamines responsible for mediating the response to acute stress.^[9]

Previous studies strongly suggested a substantial influence of peripheral sex hormones on HPA-axis response to stress with an altered endocrine stress reactivity, thus proposing a multifactorial chronic stress response in females, where they exhibited adverse effects that could not be moderated by stressor controllability. Therefore,

the current study was based on male rats to eliminate this differential body response.^[10,11,12]

Licorice (*Glycyrrhiza glabra* Linn) of the family Leguminosae grows in the Mediterranean countries and Western Asia, where its root extract has been used as a cold beverage in those areas.^[13] Licorice is mainly composed of flavonoids (such as liquiritin and isoliquiritin), isoflavonoids, chalcones (such as licochalcones A and C), and saponins such as glycyrrhizin and its aglycone; glycyrrhetic acid^[13,14] Licorice is considered one of the most commonly used herbal extracts in traditional medicine for the treatment of many respiratory, cardiovascular, gastrointestinal, genitourinary, ocular, and dermal diseases^[15,16] Many published studies have documented the anti-inflammatory, antiviral, antimicrobial, and anticancer effects of licorice. Nevertheless, antioxidant, anti-atherosclerotic, and cardioprotective activities of licorice have been reported as well.^[14,17]

Taken altogether, it is very important to explore the possible damaging effects of chronic stress on the adrenal cortex and to propose agents that could alleviate that damaging effect. Therefore, this work aimed to make a biochemical, histological, and immunohistochemical assessment of the influence of CUMS on the adrenal cortex of adult male albino rat and the possible ameliorating role of licorice aqueous extract.

MATERIAL AND METHODS

Twenty-four adult (3 months old) male albino rats, weighing 160-180 grams each, were kept standard housing conditions for 2 weeks before starting the study. The study was approved by the Research Ethics Committee of Tanta Faculty of Medicine, Egypt.

The rats were allocated into four equal groups in a random manner.

Group I (Control group): Rats were equally subdivided into 2 subgroups; subgroup Ia: the animals were kept without exposure to any stressors for 4 weeks. Subgroup Ib: the animals were kept without experiencing any stressors while being orally administered 1ml of distilled water daily for 4 weeks.

Group II (Licorice-treated group): Rats were orally administered 300 mg/kg of body weight of licorice aqueous extract dissolved in 1ml of distilled water daily for 4 weeks.^[18] The licorice was obtained from local commercial sources as a coarse black powder. An aqueous extract of licorice was prepared as previously described by Huo *et al.*^[18] with some modifications. Briefly, 200 g of licorice powder was suspended in 3 L of distilled water then the mixture was boiled with occasional stirring for 30 min. The obtained extract was then centrifuged at 8000 g for 10 min to collect the supernatant, which was then filtered and concentrated on a steam bath and finally kept at -20°C until use.

Group III (CUMS group): Rats of this group were exposed to CUMS for 4 weeks; the stress procedure

was designed according to previous studies with some modifications.^[5,19] The following 8 stressors were used; food deprivation (24 hours), water deprivation (24 hours), inversion of day/night light cycle (light-on in the night and light-off in the daytime, 24 hours), wet bedding (200 ml of water added to 300 g sawdust bedding, 12 hours), clipping the tail with forceps (1 min, the upper 1/3 of the tail), forced swimming (4°C cold water for 6 min), exposure to a foreign object (stone) for 12 hours and cage tilting at 45° for 12 hours (Table 1). The stressors were repeated in a random unpredictable pattern.

Group IV (Licorice & CUMS group): Rats of this group were orally administered licorice aqueous extract while being exposed to CUMS as described in groups II and III respectively.

Table 1: The stressors used in conducting CUMS

Stressor	period	Stressor	period
food deprivation	24 hours	clipping the tail with forceps	1 minute
water privation	24 hours	forced swimming (4°C water)	6 minutes
Inversion of day/night light cycle	24 hours	exposure to a foreign object	12 hours
wet bedding	12 hours	cage tilting	12 hours

The rats were eventually weighed and blood samples were obtained for the hormonal assay. The animals were then euthanized with pentobarbital (40 mg/kg).^[20] The adrenal gland was rapidly dissected out, weighed, and processed for biochemical study and light microscopy.

Biochemical study

The mean plasma level of aldosterone was measured by radioimmunoassay (DPC, Los Angeles, CA, USA), and the mean plasma level of corticosterone was determined using a radioimmunoassay kit (MP Biochemicals, NY, USA).

Tissue malondialdehyde (MDA) level, as a pro-oxidative marker, was detected through spectrophotometry.^[21] The antioxidant markers; Reduced glutathione (GSH) concentration^[22] and superoxide dismutase (SOD) activity^[23] were assayed. Tissue myeloperoxidase (MPO) activity was recorded using a commercial ELISA kit (Bioxytech MPO-EIA, USA) as an inflammatory index.^[24]

Preparation for light microscopy examination

Adrenal gland specimens were fixed in 10% neutral buffered formalin, washed, dehydrated, cleared, and paraffinized. Sections of 5 µm thickness were stained with hematoxylin & eosin (H&E)^[25] and Masson's trichrome stain.^[26]

Immunohistochemical staining

Prepared sections of 5 µm thickness were blocked and incubated with the primary antibodies; activated caspase-3 (ab2302; Abcam, USA) and proliferating cell nuclear antigen (PCNA) (sc-56, Santa Cruz Biotech, USA) then

incubated with the corresponding biotinylated IgG for 60 min at room temperature followed with streptavidin-biotin-horseradish peroxidase complex for another 60 min. 3,3'-diaminobenzidine (DAB) hydrogen peroxide was used to visualize the immunoreactivity. Counterstaining was applied using Mayer's hematoxylin. Negative controls were done by excluding the primary antibodies.^[27] Positive controls of activated caspase-3 and PCNA were human tonsil and rat spleen respectively.

Morphometric analysis

A light microscope (DM500, Leica, Switzerland) coupled with a digital camera (ICC50, Leica, Switzerland) was used for image acquisition. The software "ImageJ" (version 1.48v National Institute of Health, USA) was used for image analysis. Ten different non-overlapping randomly selected fields from each slide were examined at a magnification of 400 to quantitatively evaluate:

1. Mean thickness of the whole adrenal cortex (μm) and mean thickness percentage (%) of each zone (in H&E-stained sections).
2. Mean area percentage of the collagen fibers content (in Masson's trichrome-stained sections).^[28]
3. Mean percentage of caspase-3 immunohistochemical positive cells (Apoptosis index) (in DAB-stained sections) calculated as the number of positive cells \times 100 / total number of cells.^[28]
4. Mean percentage of PCNA immunohistochemical positive cells (Proliferation index) (in DAB-stained sections) calculated as the number of positive cells \times 100 / total number of cells.^[28]

Statistical analysis

The data were analyzed using one-way analysis of variance (ANOVA) followed by Tukey's test using IBM SPSS Statistics for Windows (IBM Corp, Version 22.0. Armonk, NY, USA). Differences were regarded as significant if probability value $p < 0.05$.^[29]

RESULTS

No death or mortality was recorded among the rats of the different groups during the present study.

Total body weight

The mean total body weight of rats from group III (174.57 \pm 10.99) recorded a non-significant reduction compared to control (176.93 \pm 11.78). Similarly, rats from group IV (175.89 \pm 10.21) revealed a non-significant difference from both groups I and III (Table 2).

Adrenal gland weight

The mean adrenal gland weight of rats from group III (35.33 \pm 5.21) recorded a significant reduction compared to control (39.1 \pm 3.21), whereas, group IV (37.96 \pm 5.66) revealed a significant elevation compared to group III,

which represented a non-significant difference from control (Table 2).

Biochemical findings

Both mean plasma aldosterone and corticosterone in group III (8.98 \pm 1.17, 322.19 \pm 29.27 respectively) revealed a significant elevation compared to control (6.57 \pm 1.32, 187.23 \pm 12.67 respectively), while a significant reduction was detected in group IV (7.79 \pm 1.09, 211.31 \pm 18.39 respectively) compared to group III, which still represented a significant increase compared to control (Table 2).

Both mean MDA and MPO levels in the adrenal tissue of group III revealed a significant elevation (183.04 \pm 8.51, 8.84 \pm 1.99 respectively) compared to control (96.49 \pm 5.01, 4.33 \pm 0.08 respectively), this increase has coupled with a significant reduction of both mean reduced GSH and SOD in the adrenal tissue of group III (19.39 \pm 2.08, 20.93 \pm 1.36 respectively) compared to control (42.66 \pm 4.02, 33.39 \pm 2.97 respectively). Whereas a significant difference was detected in group IV (102.15 \pm 9.49, 5.04 \pm 1.09, 37.09 \pm 7.93, 29.91 \pm 6.33 respectively) compared to group III, which denoted a non-significant difference between group IV and control (Table 2).

H&E staining

Group I (the control group) and Group II (licorice-treated group)

Examination of H&E-stained sections of the adrenal gland cortex from both groups I&II revealed the normal histoarchitecture of the adrenal cortex. The adrenal gland was surrounded by a connective tissue capsule. The zona glomerulosa (ZG) was formed of closely packed small cells with deeply stained nuclei arranged as arched clusters with blood sinusoids in between. The zona fasciculata (ZF) was composed of large cells with pale vacuolated cytoplasm and vesicular nuclei organized in straight cords with blood sinusoids in between. Zona reticularis (ZR) was composed of small darkly stained cells arranged in anastomosing cords. Blood sinusoids were observed between the cords (Figures 1,2,3).

Group III (CUMS group)

Sections of the adrenal cortex from CUMS group depicted focal capsular indentation, thickening, and subcapsular hyperplasia. The sections revealed disruption of the histoarchitecture of ZG and ZF with an intermediate cellular zone recognized between them. An apparent reduction of thickness of ZG and ZR was associated with an apparent elevation of thickness of ZF. Occasional mononuclear cellular infiltration extending through ZF was encountered (Figure 4). Congested sinusoids and scattered brown granules were detected in all three zones (Figures 5,6).

Higher magnification revealed the disturbance in the arrangement of ZG cells. Some cells showed cytoplasmic vacuolation and others showed pyknotic nuclei. Multiple irregular-shaped nuclei were observed (Figure 7). Whereas

ZF depicted large pale cells with abundant intracytoplasmic lipid droplets and dark-stained nuclei. Other cells showed cytoplasmic vacuolation. Cells with karyolytic nuclei were detected (Figure 8). Moreover, ZR revealed some vacuolated cells and some karyolytic nuclei together with some mononuclear cells (Figure 9).

Group IV (Licorice & CUMS group)

Sections of the adrenal cortex from licorice & CUMS group revealed an apparently normal histoarchitecture and thickness of the capsule, ZG, ZF, and ZR of the adrenal cortex, yet a few vacuolated cells were observed in ZG with no signs of mononuclear cellular infiltration, congested sinusoids or brown granules encountered (Figures 10,11,12).

The mean thickness of the whole adrenal cortex (μm) in group III (204.33 ± 29.01) revealed a significant reduction compared to control (254.51 ± 25.11). While group IV (243.67 ± 30.18) recorded a significant elevation regarding to group III, yet group IV presented a non-significant difference from control (Table 3, Histogram 1). Additionally, the mean thickness percentage of individual zones (relative to the total thickness) revealed a significant reduction of both ZG ($10.69 \pm 2.01\%$) and ZR ($15.29 \pm 5.99\%$) of group III compared to ZG ($11.34 \pm 2.05\%$) and ZR ($27.35 \pm 5.37\%$) of control coupling with a significant elevation in ZF of group III ($74.02 \pm 12.88\%$) compared to ZF of control ($61.31 \pm 10.11\%$). While a significant difference was recorded between all zones of group IV; ZG ($10.98 \pm 3.07\%$), ZF ($63.81 \pm 16.03\%$), ZR ($25.21 \pm 6.34\%$) and those of group III, yet these changes in group IV denoted a non-significant difference from control (Table 3, Histogram 1).

Masson's trichrome staining

Examination of Masson's trichrome-stained sections of the adrenal gland cortex from both groups I&II revealed few bluish-green collagen fibers located in the adrenal gland capsule (Figure 13). Sections from CUMS group depicted excessive collagen deposition in the adrenal capsule and both ZG and ZF (Figure 14). While sections from licorice & CUMS group showed few collagen fibers in the adrenal capsule (Figure 15).

The mean area percentage of collagen fibers content in group III (10.19 ± 2.03) revealed a significant elevation regarding to control (4.63 ± 0.95), while a significant reduction was recorded in group IV (5.11 ± 1.52) compared to group III, which represented a non-significant difference from control (Table 3, Histogram 2).

Caspase-3 immunohistochemical staining

Caspase-3-immunohistochemical-stained sections from control group I depicted few caspase-3 positive cells with a moderate nuclear and/or cytoplasmic reaction presented as a brownish coloration in all three

zones of adrenal cortex (Figures 16,17). While group III revealed numerous caspase-3-positive cells with a strong nuclear and/or cytoplasmic reaction in ZG, ZF, and ZR (Figures 18,19). Whereas, group IV displayed some caspase-3-positive cells with a moderate nuclear and/or cytoplasmic reaction in ZG, while only a few positive cells could be observed in both ZG and ZR (Figures 20,21).

The mean percentage of caspase-3-immunopositive cells recorded a significant elevation in group III (17.55 ± 2.56) compared to control (5.98 ± 0.93), while group IV (7.21 ± 1.91) showed a significant reduction compared to group III and a non-significant difference from control (Table 3, Histogram 2).

PCNA immunohistochemical staining

PCNA-immunohistochemical-stained sections from control group I revealed few PCNA-positive cells with a moderate nuclear reaction presented as a brownish coloration mainly in the junctional zone between ZG and ZF and in ZF with few positive cells detected in ZG, while none was detected in ZR (Figures 22,23). Meanwhile, group III showed many PCNA-positive cells with a strong nuclear reaction mainly in the junctional zone between ZG and ZF and in ZF, while few positive cells were detected in both ZG and ZR (Figures 24,25). Whereas group IV depicted some PCNA-positive cells with a moderate nuclear reaction mainly in the junctional zone between ZG and ZF and in ZF, few positive cells were detected in ZG, while almost none could be detected in ZR (Figures 26,27).

The mean percentage of PCNA-immunopositive cells revealed a significant elevation in group III (15.38 ± 3.69) regarding to control (10.29 ± 1.14), whereas group IV (11.61 ± 2.59) showed a significant reduction compared to group III, which represented a non-significant difference from control (Table 3, Histogram 2).

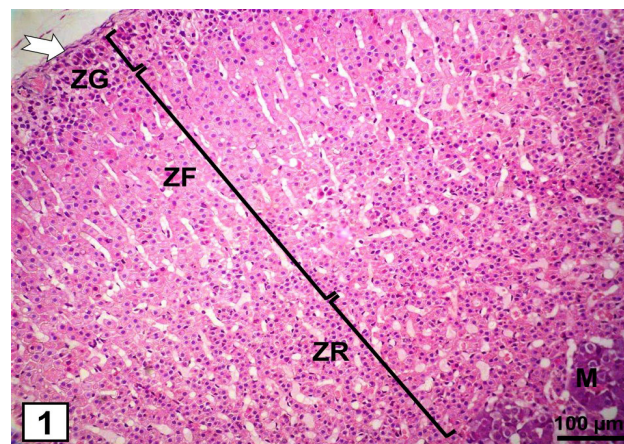


Fig. 1: A photomicrograph of the adrenal gland from control group shows a normal histoarchitecture of the adrenal cortex three distinct zones; zona glomerulosa (ZG), zona fasciculata (ZF) and zona reticularis (ZR). The adrenal gland is surrounded by a connective tissue capsule (notched arrow). Notice part of the adrenal medulla (M) (H&E x200, scale bar=100 μm).

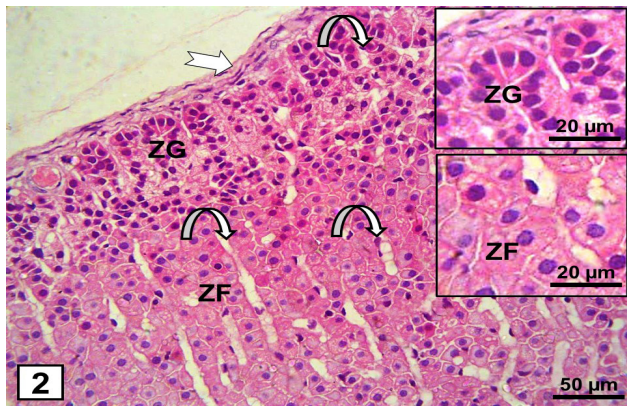


Fig. 2: A photomicrograph of the adrenal gland from control group shows zona glomerulosa (ZG) closely packed cells with deeply stained nuclei arranged as arched clusters under the adrenal gland capsule (notched arrow) with blood sinusoids in between (curved arrow). The cells of zona fasciculata (ZF) are large cells with pale vacuolated cytoplasm and vesicular nuclei organized in straight cords with blood sinusoids in between (curved arrows). (H&E x400, scale bar=50 µm, insets x1000, scale bar=20 µm).

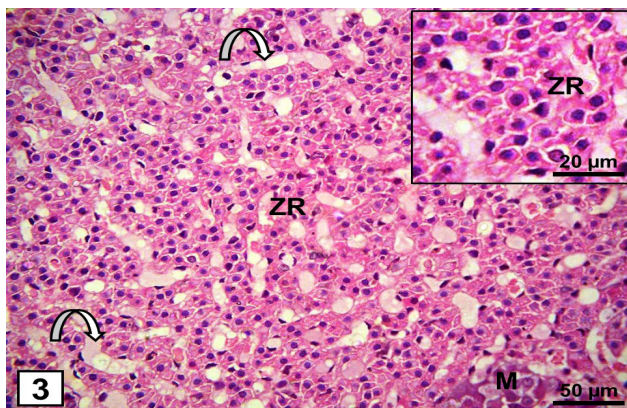


Fig. 3: A photomicrograph of the adrenal gland from control group shows the small darkly stained cells of zona reticularis (ZR) arranged in anastomosing cords. Blood sinusoids (curved arrows) are observed between the cords. Notice part of the adrenal medulla (M) (H&E x400, scale bar=50 µm, insets x1000, scale bar=20 µm).

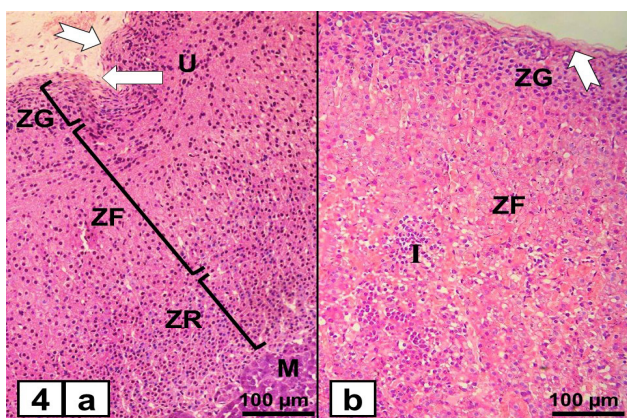


Fig. 4: Photomicrographs of the adrenal gland from CUMS group shows in [a, b] focal indentation (thick arrow), and thickening (notched arrows) with subcapsular hyperplasia. Disruption of the regular architectural pattern of ZG and ZF is associated with an apparent decrease in thickness of ZG & ZR and an apparent increase in the thickness of ZF. Notice an intermediate cellular zone (U) between ZG & ZF and a part of the adrenal medulla (M) [b] A mononuclear infiltration (I) extending through ZF is observed. (H&E x200, scale bar=100 µm).

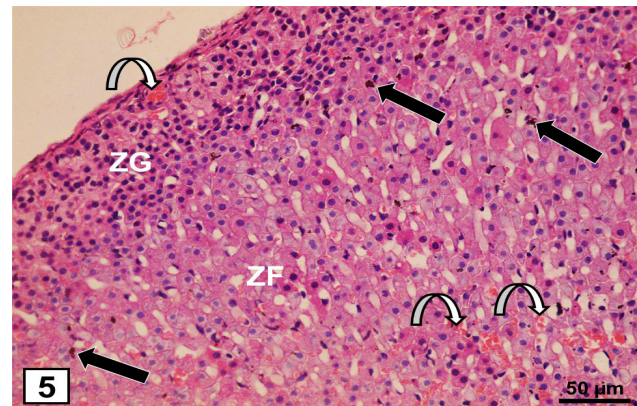


Fig. 5: A photomicrograph of the adrenal gland from CUMS group shows disruption of the histoarchitectural pattern of ZG and ZF. Notice congested sinusoids (curved arrows) and scattered brown granules (thick arrows) in both ZG and ZF. (H&E x400, scale bar=50 µm).

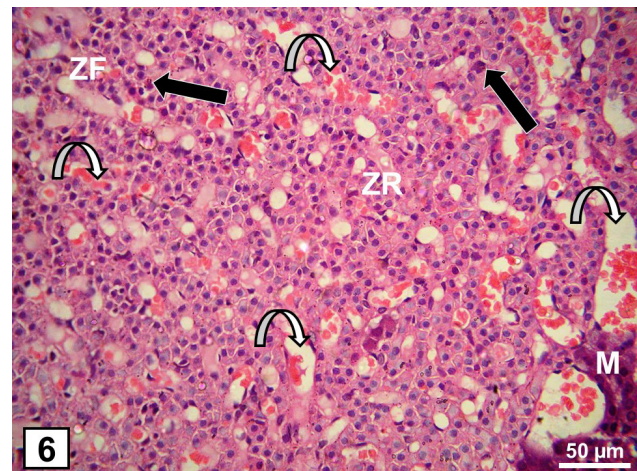


Fig. 6: A photomicrograph of the adrenal gland from CUMS group shows disruption of the histoarchitectural pattern of ZF. Congested sinusoids (curved arrows) and scattered brown granules (thick arrows) are observed in both ZF and ZR. Notice part of the adrenal medulla (M) (H&E x400, scale bar=50 µm).

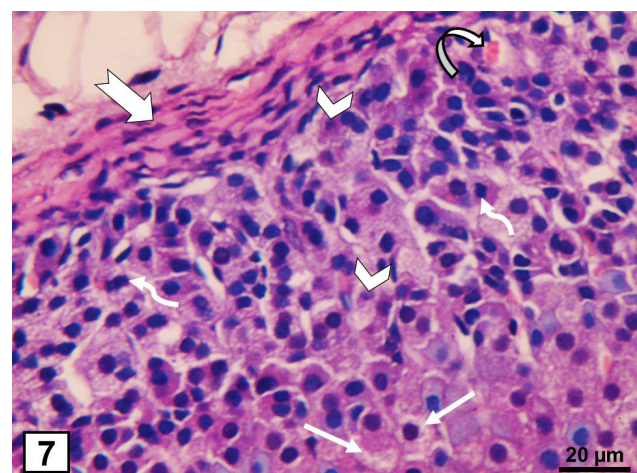


Fig. 7: A photomicrograph of the adrenal gland from CUMS group shows thickened adrenal capsule (notched arrow) and a disrupted arrangement of the cells of ZG. Some cells show cytoplasmic vacuolation (thin arrows) and others show pyknotic nuclei (arrowheads). Multiple irregular-shaped nuclei are observed (wavy arrows). Notice few congested sinusoids (curved arrow). (H&E x1000, scale bar=20 µm).

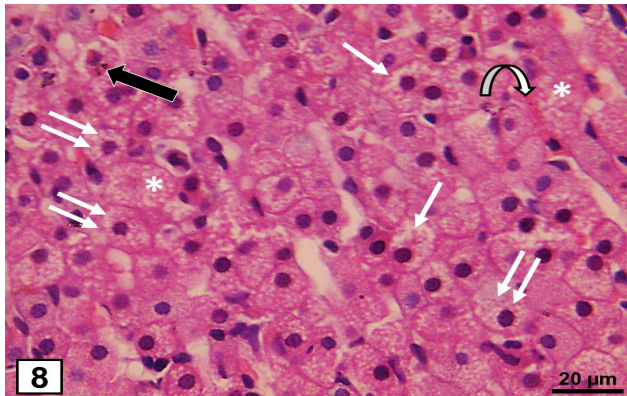


Fig. 8: A photomicrograph of the adrenal gland from CUMS group shows disrupted arrangement of the cells of ZF. Most cells appear large pale with abundant intracytoplasmic vacuoles and dark-stained nuclei (double thin arrows). Other cells show cytoplasmic vacuolation (thin arrow). Cells with karyolytic nuclei can be observed (asterisks). Few congested sinusoids (curved arrow) and scattered brown granules (thick arrow) are detected. (H&E x1000, scale bar=20 μm).

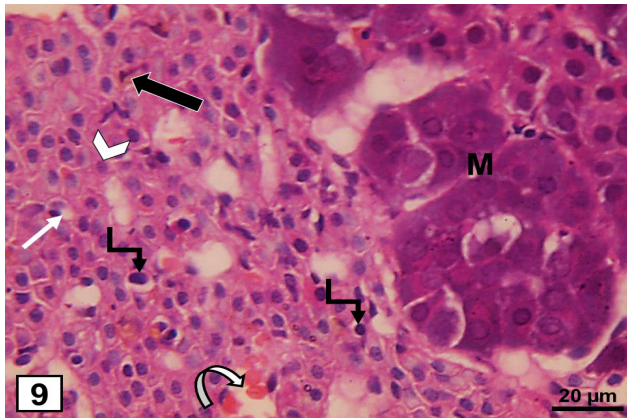


Fig. 9: A photomicrograph of the adrenal gland from CUMS group shows ZR with vacuolated cells (thin arrow), other cells show karyolytic nuclei (arrowhead). Mononuclear cells (angular arrows), congested sinusoids (curved arrow), and scattered brown granules (thick black arrow) are detected. Notice part of the adrenal medulla (M) (H&E x1000, scale bar=20 μm).

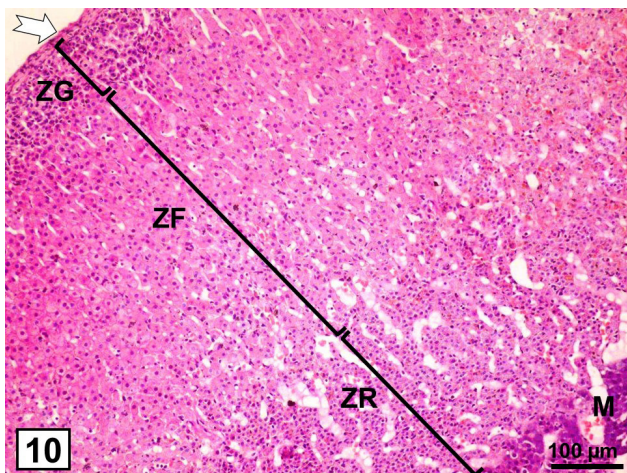


Fig. 10: A photomicrograph of the adrenal gland from licorice & CUMS group shows an apparently normal histological architecture and thickness of capsule (notched arrow), zona glomerulosa (ZG), fasciculata (ZF) and reticularis (ZR) of the adrenal cortex. Notice part of the adrenal medulla (M) (H&E x200, scale bar=100 μm).

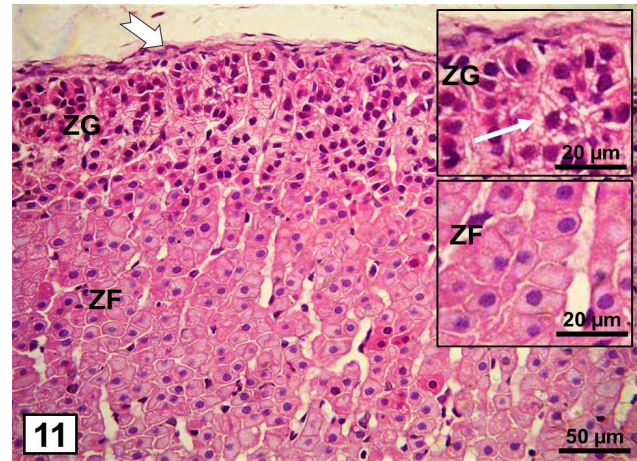


Fig. 11: A photomicrograph of the adrenal gland from licorice & CUMS group shows an apparently normal histoarchitecture and thickness of capsule (notched arrow), zona glomerulosa (ZG), fasciculata (ZF) and reticularis (ZR) of the adrenal cortex. Few vacuolated cells (thin arrow) are observed in ZG (H&E x400, scale bar=50 μm, insets x1000, scale bar=20 μm).

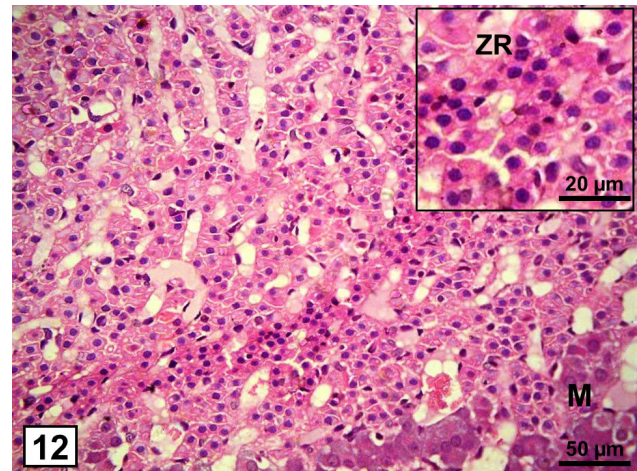


Fig. 12: A photomicrograph of the adrenal gland from licorice & CUMS group shows a near-normal architecture of zona reticularis (ZR). Notice part of the adrenal medulla (M) (H&E x400, scale bar=50 μm, insets x1000, scale bar=20 μm).

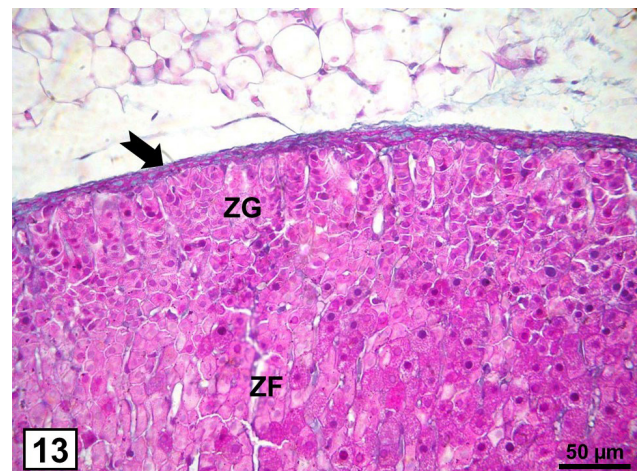


Fig. 13: A photomicrograph of the adrenal gland from control group shows few bluish-green collagen fibers of the adrenal gland capsule (notched arrow). (Masson's trichrome x400, scale bar=50 μm)

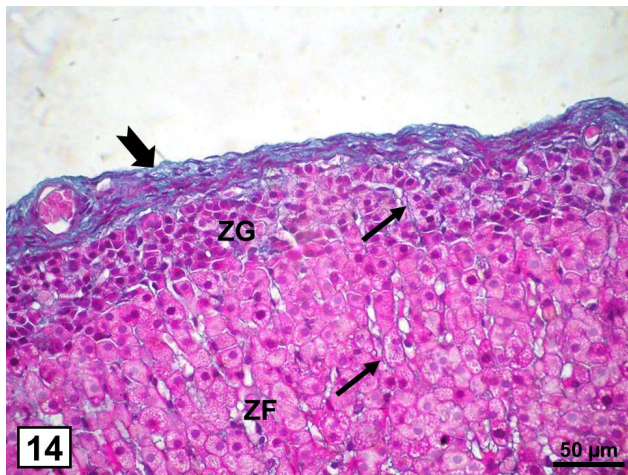


Fig. 14: A photomicrograph of the adrenal gland from CUMS group shows excessive bluish-green collagen fibers deposition (thin arrows) in the adrenal gland capsule (notched arrow), zona glomerulosa (ZG), and fasciculata (ZF) (Masson's trichrome x400, scale bar=50 μm)

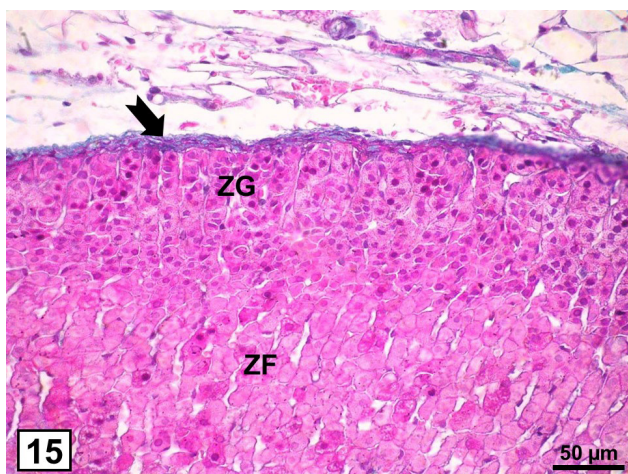


Fig. 15: A photomicrograph of the adrenal gland from licorice & CUMS group shows few collagen fibers in the adrenal gland capsule (notched arrow). (Masson's trichrome x400, scale bar=50 μm)

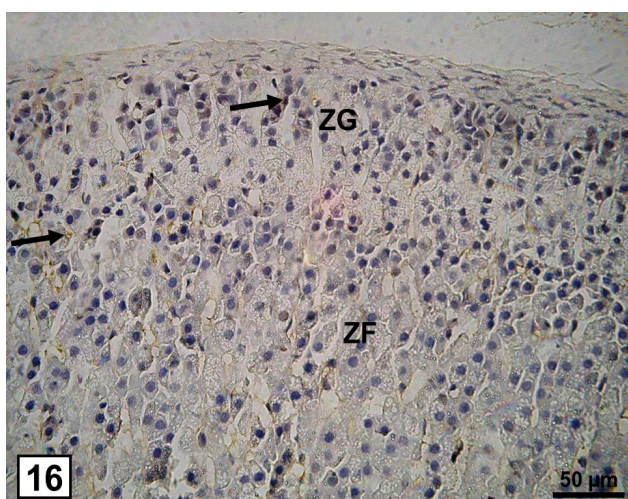


Fig. 16: A photomicrograph of the adrenal gland from control group shows few caspase-3 positive cells with a moderate nuclear and/or cytoplasmic reaction as a brownish coloration (arrows) in ZG and ZF. (Caspase-3x400, scale bar=50 μm)

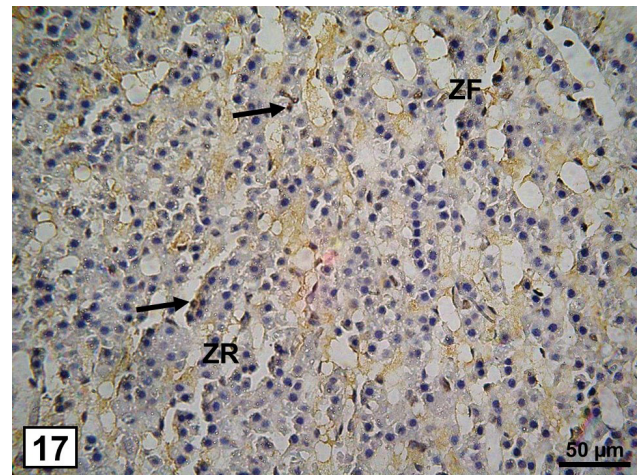


Fig. 17: A photomicrograph of the adrenal gland from control group shows few caspase-3 positive cells with a moderate nuclear and/or cytoplasmic reaction (arrows) in ZF and ZR. (Caspase-3x400, scale bar=50 μm)

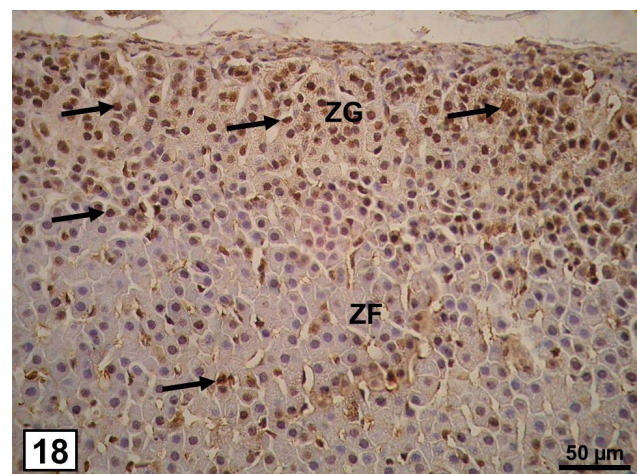


Fig. 18: A photomicrograph of the adrenal gland from CUMS group shows numerous caspase-3 positive cells with a strong nuclear and/or cytoplasmic reaction (arrows) in ZG and ZF. (Caspase-3x400, scale bar=50 μm)

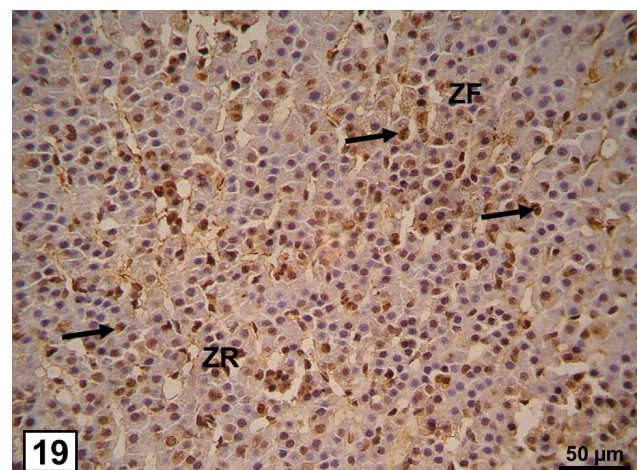


Fig. 19: A photomicrograph of the adrenal gland from CUMS group shows numerous caspase-3 positive cells with a strong nuclear and/or cytoplasmic reaction (arrows) in the ZF and ZR. (Caspase-3x400, scale bar=50 μm)

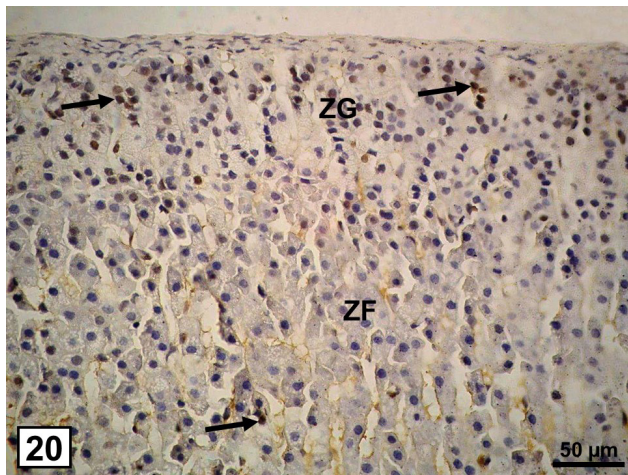


Fig. 20: A photomicrograph of the adrenal gland from licorice & CUMS group shows some caspase-3 positive cells with a strong nuclear and/or cytoplasmic reaction (arrows) mainly in ZG, few positive cells are observed in ZF. (Caspase-3x400, scale bar=50 μm)

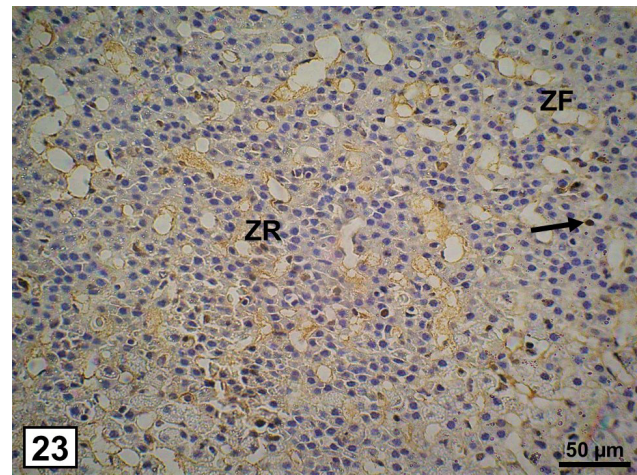


Fig. 23: A photomicrograph of the adrenal gland from control group shows few PCNA positive cells with a moderate nuclear reaction (arrows) mainly in ZF, while none can be detected in ZR. (PCNAx400, scale bar=50 μm)

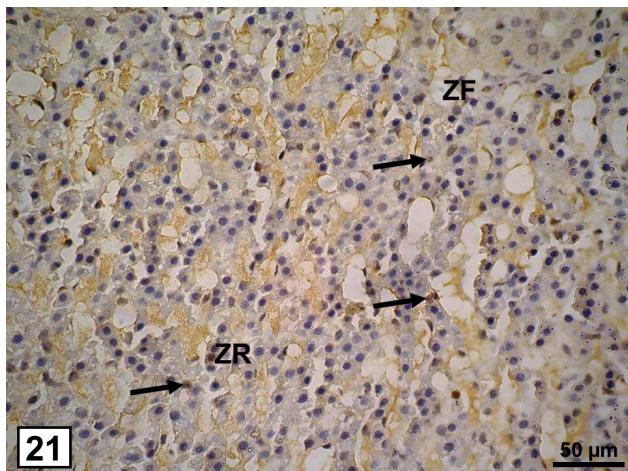


Fig. 21: A photomicrograph of the adrenal gland from licorice & CUMS group shows few caspase-3 positive cells with a moderate nuclear and/or cytoplasmic reaction (arrows) in ZF and ZR. (Caspase-3x400, scale bar=50 μm)

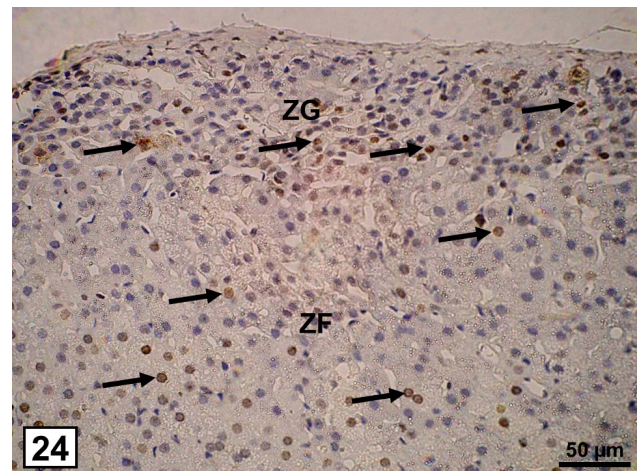


Fig. 24: A photomicrograph of the adrenal gland from CUMS group shows many PCNA positive cells with a strong nuclear reaction (arrows) mainly in the junctional zone between ZG and ZF and in ZF, few positive cells are observed in ZG. (PCNAx400, scale bar=50 μm)

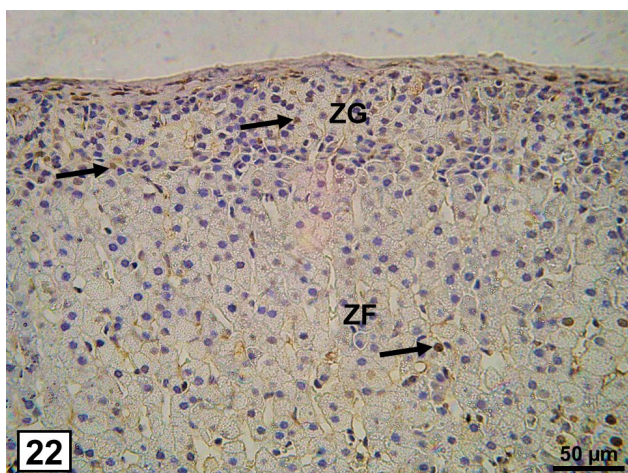


Fig. 22: A photomicrograph of the adrenal gland from control group shows few PCNA positive cells with a moderate nuclear reaction in the form of a brownish coloration (arrows) mainly in the junctional zone between ZG and ZF and in ZF, few positive cells are detected in ZG. (PCNAx400, scale bar=50 μm)

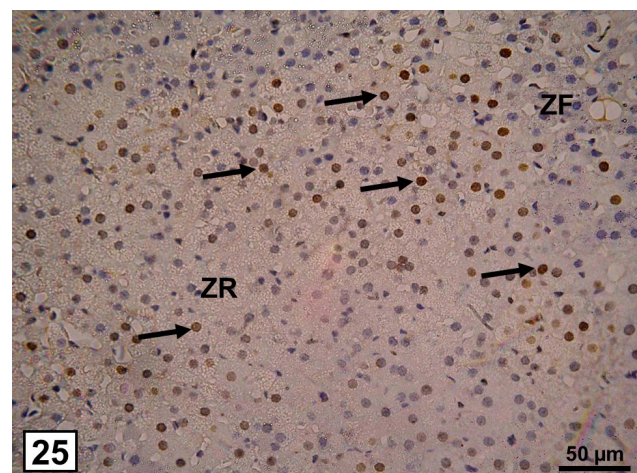


Fig. 25: A photomicrograph of the adrenal gland from CUMS group shows many PCNA positive cells with a strong nuclear reaction (arrows) mainly in ZF, while few positive cells are detected in ZR. (PCNAx400, scale bar=50 μm)

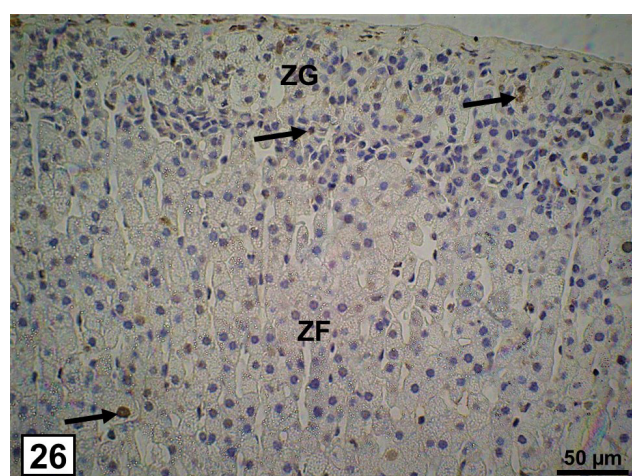


Fig. 26: A photomicrograph of the adrenal gland from licorice & CUMS group shows some PCNA positive cells with a moderate nuclear reaction (arrows) mainly in the junctional zone between ZG and ZF and in ZF, few positive cells are detected in ZG. (PCNAx400, scale bar=50 μm)

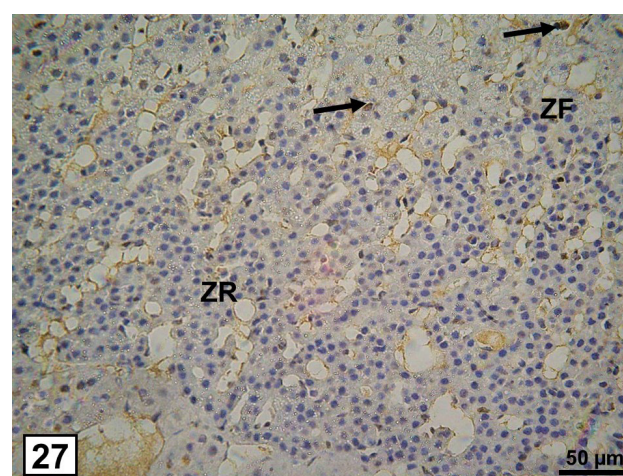


Fig. 27: A photomicrograph of the adrenal gland from licorice & CUMS group shows some PCNA positive cells with a moderate nuclear reaction (arrows) mainly in ZF, while almost none are detected in ZR. (PCNAx400, scale bar=50 μm)

Table 2: Biometric and biochemical analysis of adrenal gland different parameters

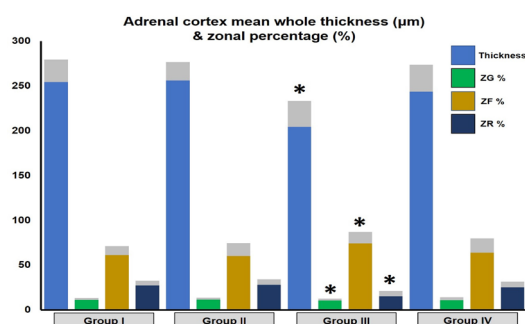
Parameters	Group I	Group II	Group III	Group IV
Mean total body weight (g)	176.93±11.78	176.29±11.26	174.57±10.99	175.89±10.21
Mean adrenal weight (mg)	39.1±3.21	38.95±3.91	35.33±2.21 ^{a,b}	37.96±3.16 ^c
Plasma aldosterone (ng/dl)	6.57±1.32	6.15±1.01	8.98±1.17 ^{a,b}	7.79±1.09 ^{a,b,c}
Plasma corticosterone (ng/ml)	187.23±12.67	187.36±11.09	322.19±29.27 ^{a,b}	211.31±18.39 ^{a,b,c}
MDA nmol/g tissue protein	96.49±5.01	96.72±5.14	183.04±8.51 ^{a,b}	102.15±9.49 ^c
Reduced GSH mol/g tissue protein	42.66±4.02	42.39±4.01	19.39±2.08 ^{a,b}	37.09±7.93 ^c
SOD U/g of tissue protein	33.39±2.97	33.24±2.90	20.93±1.36 ^{a,b}	29.91±6.33 ^c
MPO ng/mg tissue protein	4.33±0.08	4.51±0.01	8.84±1.99 ^{a,b}	5.04±1.09 ^c

Data is expressed as mean ± standard deviation. a $p < 0.05$ vs group I, b $p < 0.05$ vs group II, c $p < 0.05$ vs group III.

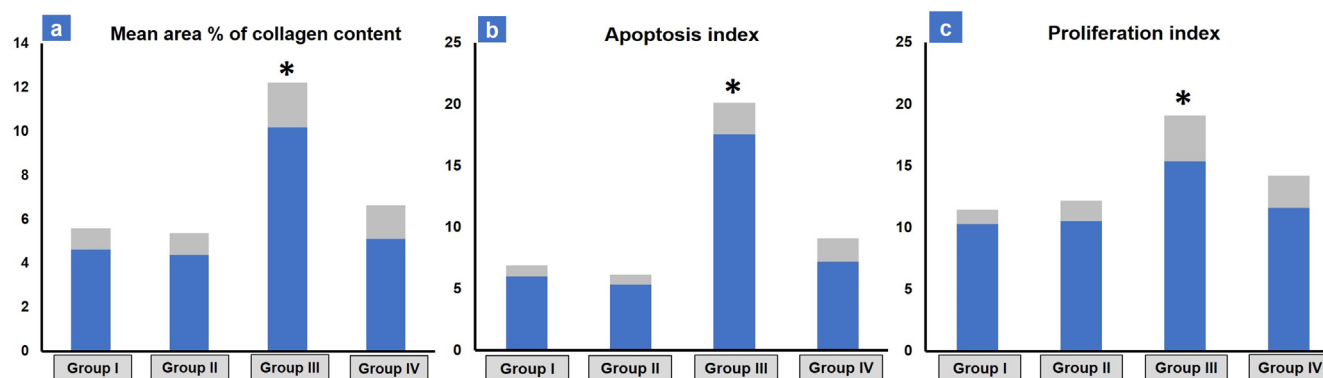
Table 3: Statistical analysis of adrenal cortex different parameters

Parameters	Group I	Group II	Group III	Group IV
Mean thickness of the whole adrenal cortex (μm)	254.51±25.11	256.39±20.31	204.33±29.01 ^{a,b}	243.67±30.18 ^c
Mean thickness percentage (%) of each zone (relative to the total thickness)				
Zona Glomerulosa	11.34±2.05	11.69±2.19	8.69±1.01 ^{a,b}	10.98±3.07 ^c
Zona Fasciculata	61.31±10.11	60.11±14.31	74.02±12.88 ^{a,b}	63.81±16.03 ^c
Zona Reticularis	27.35±5.37	28.2±6.11	17.29±5.99 ^{a,b}	25.21±6.34 ^c
Mean area percentage (%) of the collagen fibers content	4.63±0.95	4.38±1.01	10.19±2.03 ^{a,b}	5.11±1.52 ^c
Mean percentage (%) of caspase-3-positive cells (Apoptosis index)	5.98±0.93	5.34±0.81	17.55±2.56 ^{a,b}	7.21±1.91 ^c
Mean percentage (%) of PCNA-positive cells (Proliferation index)	10.29±1.14	10.55±1.62	15.38±3.69 ^{a,b}	11.61±2.59 ^c

Data is expressed as mean ± standard deviation. a $p < 0.05$ vs group I, b $p < 0.05$ vs group II, c $p < 0.05$ vs group III.



Histogram 1: Morphometric analysis of mean thickness of the whole adrenal cortex (μm) and mean thickness percentage (%) of each zone (relative to the total thickness); (ZG) Zona glomerulosa, (ZF) Zona Fasciculata, (ZR) Zona Reticularis. * indicates significance versus control group.



Histogram 2: Morphometric analysis of; a] Mean area percentage (%) of the collagen fibers content, b] Mean percentage (%) of caspase-3-positive cells (Apoptosis index), c] Mean percentage (%) of PCNA-positive cells (Proliferation index). * indicates significance versus control group.

DISCUSSION

CUMS is a trusted model of depression for its reliable validity. In the used model of CUMS, the animals were exposed to variable stressors such as water deprivation, food deprivation, tilted cages, and continuous illumination for them to develop a group of changes that mimic symptoms of depression in humans such as sleep disturbance, altered diurnal rhythm, and anhedonia.^[1]

In the present work, animals from the CUMS group recorded a non-significant reduction of the total body weight as compared to control as was similarly reported by other researchers who considered this lack of body weight changes as proof for the mild nature of the stressors used in the model.^[30] However, a significant reduction of the weight of the adrenal glands of CUMS group was reported. This finding was also observed by others who attributed this weight decrease to the decreased cellularity and the dilated intercellular spaces in the adrenal cortex.^[31] Moreover, this significant reduction of adrenal weight in the CUMS group in the present work was coupled with a significant reduction of thickness of the whole adrenal cortex together with a significant reduction of thickness of both ZG and ZR associated with a significant elevation in the thickness of ZF as compared to control. Similar findings were reported by another work that suggested the differential impact of chronic stress on the adrenocortical zones in the form of growth of ZF and atrophy of ZG.^[8] Furthermore, they illustrated that the growth of ZF was caused by both hyperplasia in its outer part and hypertrophy in its inner part while atrophy of ZG was caused by the decrease in their cell size.

In the present work, CUMS group recorded a significant elevation of both serum aldosterone and corticosterone levels as compared to control. Researchers attributed this increase in aldosterone level to the stimulation of renin-angiotensin system secondary to stress.^[30] Whereas the increase in corticosterone serum level could be explained according to other researchers who illustrated that at the beginning of exposure to stress, there is negative feedback by the elevated levels of cortisol on the production of corticotropin releasing hormone from the hypothalamus to decrease the cortisol secretion from the adrenal cortex.

However, later with the chronic exposure to stress, that negative feedback fails to control the cortisol secretion and its levels increase markedly reaching seriously dangerous levels that eventually result in neuroendocrine, cardiovascular, and immune disorders.^[32]

Biochemical assay in the current work revealed a significant increase in the pro-oxidant marker MDA in the CUMS group associating with a significant elevation of both reduced GSH and SOD antioxidant markers as compared to control. The combined elevation of reactive oxygen species level with dropped antioxidant enzymes causes defective antioxidant defenses and lipid peroxidation, which strongly suggest oxidative stress as a possible mechanism of the adverse effects of chronic stress on different cellular functions. Moreover, oxidative stress is currently considered a key mechanism in development of depression in both humans and rodents.^[33]

Histological examination of the CUMS group revealed thickening of the adrenal gland capsule, which was similarly reported in both adult and senile stressed rats.^[9] A previous study argued that the subcapsular hyperplasia originates from the cells of ZG and its incidence could increase under stressful conditions.^[34] Additionally, congested sinusoids were detected in the CUMS group, this finding coincided with the work of other researchers who attributed it to the increased vascular demand to adapt to the increased endocrinal activity and hormonal secretions of the adrenal cortex in response to stress.^[35] Nevertheless, the CUMS group also revealed occasional mononuclear cellular infiltration in some sections in association with an increased MPO level in adrenal tissue. Similar results were reported by another work that documented the occurrence of intestinal mucosal inflammation secondary to chronic stress evidenced by extensive infiltration of the mucosa with activated neutrophils together with an increased expression of some pro-inflammatory mediators such as interleukin-6 (IL-6), interferon gamma (IFN- γ), and tumor necrosis factor alpha (TNF- α).^[36] Similarly, other researchers reported increased levels of IL-6, interleukin-1 beta (IL-1 β), and TNF- α in both serum and hippocampal tissues in mice subjected to chronic mild stress.^[37] A previous study could illustrate the relation between chronic

stress and systemic inflammation. They suggested that the body adapts to stress through the initiation of an immune reaction mediated via certain intercellular mediators such as TNF- α .^[38]

In the present work, cytoplasmic alterations in the form of cytoplasmic vacuolation, lipid droplets, and brown deposits in the different zones of the adrenal cortex were recorded in the CUMS group. These findings were similarly reported in another work that attributed the cytoplasmic vacuolation to the dilatation of the smooth endoplasmic reticulum involved in the synthesis of the steroid hormones. They related the abundant lipid droplets to the increased hormonal synthesis being essential precursors of the steroidal hormones, whereas their destruction might explain the brown deposits suggested to be lipofuscin pigment, and they finally explained that those changes to be signs of degeneration.^[39]

Besides, CUMS group revealed several nuclear changes in the form of irregularly shaped darkly stained, karyolytic, or pyknotic nuclei in association with a significant upregulation in both PCNA and caspase-3 immunohistochemical expression compared to control. A previous study similarly reported an increase in proliferative cells mainly confined to the ZF,^[8] which might be induced by DNA damage in absence of cell cycling.^[40] Cellular apoptosis and regeneration observed in different zones of adrenal cortex in the present work could be explained according to another work which illustrated that adrenal gland undergoes dynamic histological changes in the form of cellular death and cellular proliferation and balance between those processes must be established to maintain structure and function of adrenal gland. They reported that the cellular replacement in different adrenal cortex zones could be attributed to many theories; One theory is the migration theory which proposed that the cells proliferate in the outer part of the cortex then migrate from ZG to ZF to finally reach ZR. Another theory is the transformation theory which suggested that the cells proliferate in an intermediate zone between ZG and ZF then the cells migrate towards both the capsule and the medulla. A third theory; the zonal theory suggested that both apoptosis and cell proliferation occur independent of each other in each zone of the cortex. This means that each zone is locally regulated without affection of the function of other zones.^[41] The current findings would suggest the second theory, where an intermediate junctional cellular zone was recognized between ZG and ZF, which revealed evident upregulation of PCNA immunoeexpression.

Nevertheless, researchers proposed that the differentiation of the adrenocortical adult progenitor/stem cells and their centripetal migration eventually ended by their apoptosis at the corticomedullary junction,^[42,43] where they are removed by macrophages, which were suggested to be a paracrine regulator that provokes the corticosterone secretion.^[44] This could explain the presence of mononuclear cells deep in the adrenal cortex along with the upregulation

of caspase-3 immunoeexpression particularly in the ZR in the CUMS group in the current study.

Moreover, Fulda *et al.*^[45] illustrated that cellular stress response varies greatly according to the type, duration, and severity of the stress stimuli. They explained that the cell's first stress response would be defensive and protective in a trial to recover the cell from the injury and maintain its survival. However, chronic stress could result in activation of certain cascades that would eventually end in cell apoptosis through activation of caspases which are a family of cysteine protease enzymes that act as death effector molecules in apoptosis. Caspases are responsible for the different morphological features of apoptotic cell death such as nuclear shrinkage, irregularity of cell outlines, and loss of the normal cell shape as reported in the present work.

Licorice has been used for clinical treatment of various diseases owing to their anti-inflammatory, antimicrobial, antiulcer, expectorant, anxiolytic, and antioxidant activities.^[46]

In the present work, concomitant administration of licorice along with exposure to the stressors in group IV significantly alleviated most biochemical and histological, and immunohistochemical aspects in comparison to the CUMS group, however, it recorded a non-significant difference from control in most parameters. Licorice significantly downregulated the elevated tissue MDA level while significantly upregulated the reduced GSH and SOD levels. Such antioxidant action of licorice was similarly reported in several studies on different organs; liver, stomach, lung, testis, and kidney.^[14,18,47] Other researchers attributed this antioxidant activity of licorice to the effect of glycyrrhetic acid.^[48] Besides, Dogan *et al.*^[49] stated that licorice flavonoids exert antioxidant activity that was 100-fold stronger than that of vitamin E. This relief of oxidative stress is strongly suggested to be accountable for the favorable near-normal histological outcome of licorice co-treated group IV compared to the CUMS group.

Moreover, licorice significantly downregulated the elevated MPO adrenal level and relieved the signs of inflammation as compared to the CUMS group. Huo *et al.*^[18] proposed that licorice has an anti-inflammatory effect through downregulating the expression of some proinflammatory mediators. According to other researchers, licorice's anti-inflammatory activity could be attributed to the steroid-like activity of certain components of licorice making it similar in action to hydrocortisone. They added that some licorice constituents inhibit phospholipase A2 enzyme, cyclooxygenase activity, prostaglandin formation, and platelet aggregation which all represent critical mediators in various inflammatory processes.^[13] Moreover, licorice co-treatment significantly decreased collagen deposition compared to group III, which came per the findings of another work which reported the role of licorice in ameliorating bleomycin-induced pulmonary

fibrosis, most probably through its immunomodulatory and anti-inflammatory effects.^[50]

Licorice co-treated group IV recorded a significant reduction of the percentage of both proliferative and apoptotic cells as compared to the CUMS group. This coincided with other researches who stated that glycyrrhetic acid (GA) decreased expression of PCNA in mice fed with GA before UVB irradiation.^[51] Researchers attributed the anti-proliferative activity of licorice to GA blocking the activation of NF- κ B through interference with degradation or phosphorylation of I κ B. They added that iso-liquiritigenin (ILQ), one of licorice chalconoids, has an anti-proliferative activity as well by acting as aromatase enzyme inhibitor. Also, they noted the effect of isoangustone A, a licorice flavonoid, on the cell cycle and its anti-proliferative activity.^[52] Moreover, Fukuchi *et al.*^[53] pointed out the antitumor activity of the flavonoid components of licorice, particularly flavonoids isoliquiritigenin and neoisoliquiritin apioside exert higher anti-proliferative activity than other licorice flavonoids, however, the exact mechanism may be still unclear.

Nevertheless, the concurrent significant reduction of apoptotic cells in licorice co-treated group could be attributed to the antioxidant property of licorice evidenced through the biochemical assay in the current work, where antioxidants are strongly suggested to prevent radical-mediated cell damage thus indirectly suppressing apoptosis^[54] Moreover, the antiapoptotic activity of licochalcone C, one of licorice chalcones, was strongly proposed by Zhou *et al.*^[55] who reported that the pretreatment of ischemia/perfusion injury of rat heart with licochalcone C was able to decrease the ratio of TUNEL-positive cells, alleviate histopathological changes, and diminish the mitochondrial injury.

Nevertheless, licorice co-treated group IV recorded a significant reduction of both plasma aldosterone and corticosterone compared to the CUMS group, this agreed with previous reports suggesting the capability of licorice to downregulate corticosterone level in chronic unpredictable stress model of depression.^[56] However, licorice co-treated group IV finding still represented a significant elevation compared to control, which came in accordance with previous studies proposing that licorice could stimulate the adrenal cortex to secrete high amounts of both aldosterone and corticosterone in order to help the body dealing with stressful conditions and relieving exhaustion. They attributed this activity to the effect of glycyrrhetic acid (GA).^[52,57] The differential underlying mechanism by which licorice affects adrenal hormones in a normal, stressed, or adrenal-fatigued subject remains to be clarified.

CONCLUSION

Taken altogether, this work demonstrated the adverse effects of CUMS on the adrenal cortex regarding the redox status, morphology, apoptosis, and proliferation. Licorice proved beneficial in alleviating those adverse effects most

probably through its antioxidant, anti-inflammatory, and antiproliferative properties although licorice could not normalize down the elevated adrenal hormones levels.

We could recommend a controlled licorice intake as an adjuvant supplement during chronic stress management while monitoring aldosterone and corticosterone levels.

CONFLICT OF INTERESTS

There are no conflicts of interest.

REFERENCES

1. Abdul Shukoor MS, Baharuldin MTH Bin, Mat Jais AM, Mohamad Moklas MA, Fakurazi S. Antidepressant-Like Effect of Lipid Extract of *Channa striatus* in Chronic Unpredictable Mild Stress Model of Depression in Rats. *Evid Based Complement Alternat Med* 2016;2016:2986090.
2. Torales J, O'Higgins M, Castaldelli-Maia JM, Ventriglio A. The outbreak of COVID-19 coronavirus and its impact on global mental health. *Int J Soc Psychiatry* March 2020:0020764020915212.
3. Guan S, Liu J, Fang EF, Ng TB, Lian Y, Ge H. Chronic unpredictable mild stress impairs erythrocyte immune function and changes T-lymphocyte subsets in a rat model of stress-induced depression. *Environ Toxicol Pharmacol* 2014;37:414–22.
4. Pekala K, Budzynska B, Biala G. Utility of the chronic unpredictable mild stress model in research on new antidepressants. *Curr Issues Pharm Med Sci* 2014;27:97–101.
5. Wu G-F, Ren S, Tang R-Y, *et al.* Antidepressant effect of taurine in chronic unpredictable mild stress-induced depressive rats. *Sci Rep* 2017;7:4989.
6. Bielajew C, Konkle ATM, Merali Z. The effects of chronic mild stress on male Sprague–Dawley and Long Evans rats. *Behav Brain Res* 2002;136:583–92.
7. Febbraro F, Svenningsen K, Tran TP, Wiborg O. Neuronal substrates underlying stress resilience and susceptibility in rats. *PLoS One* 2017;12:e0179434–e0179434.
8. Ulrich-Lai YM, Figueiredo HF, Ostrander MM, Choi DC, Engeland WC, Herman JP. Chronic stress induces adrenal hyperplasia and hypertrophy in a subregion-specific manner. *Am J Physiol Metab* 2006;291:E965–73.
9. Zaki SM, Abdelgawad FA, El-Shaarawy EAA, Radwan RAK, Aboul-hoda BE. Stress-induced changes in the aged-rat adrenal cortex. Histological and histomorphometric study. *Folia Morphol (Warsz)* 2018;77:629–41.
10. Oyola MG, Handa RJ. Hypothalamic-pituitary-adrenal and hypothalamic-pituitary-gonadal axes: sex differences in regulation of stress responsivity. *Stress* 2017;20:476–94.

11. Guo L, Chen Y-X, Hu Y-T, *et al.* Sex hormones affect acute and chronic stress responses in sexually dimorphic patterns: Consequences for depression models. *Psychoneuroendocrinology* 2018;95:34–42.
12. Rincón-Cortés M, Herman JP, Lupien S, Maguire J, Shansky RM. Stress: Influence of sex, reproductive status and gender. *Neurobiol Stress* 2019;10:100155.
13. Zadeh JB, Kor ZM, Gofar MK. Licorice (*Glycyrrhiza glabra* Linn) As a Valuable Medicinal Plant. *Int J Adv Biol Biom Res* 2013;1:1281–8.
14. Abdelzaher W, Ali D, Khalil W. Could Licorice prevent Bisphenol A-Induced Biochemical, Histopathological and Genetic Effects in the Adult Male Albino Rats? *Ain Shams J Forensic Med Clin Toxicol* 2018;30:73–87.
15. Sakr SA, Shalaby SY. Carbendazim-induced testicular damage and oxidative stress in albino rats: ameliorative effect of licorice aqueous extract. *Toxicol Ind Health* 2012;30:259–67.
16. Ajagannanavar SL, Shamarao S, Battur H, Tikare S, Al-Kheraif AA, Al Sayed MSAE. Effect of aqueous and alcoholic Stevia (*Stevia rebaudiana*) extracts against *Streptococcus mutans* and *Lactobacillus acidophilus* in comparison to chlorhexidine: An *in vitro* study. *J Int Soc Prev Community Dent* 2014;4:S116–21.
17. Kataya HH, Hamza AA, Ramadan GA, Khasawneh MA. Effect of licorice extract on the complications of diabetes nephropathy in rats. *Drug Chem Toxicol* 2011;34:101–8.
18. Huo HZ, Wang B, Liang YK, Bao YY, Gu Y. Hepatoprotective and antioxidant effects of licorice extract against CCl₄-induced oxidative damage in rats. *Int J Mol Sci* 2011;12:6529–43.
19. Deng X-Y, Xue J-S, Li H-Y, *et al.* Geraniol produces antidepressant-like effects in a chronic unpredictable mild stress mice model. *Physiol Behav* 2015;152:264–71.
20. Gaertner DJ, Hallman TM, Hankenson FC, Batchelder MA. Anesthesia and analgesia for laboratory rodents. In: Fish, R.E., Danneman, P.J., Brown, M., Karas AZ, editor. *Anesthesia and Analgesia in Laboratory Animals*. 2nd ed. Elsevier Academic Press, London (UK); 2008:239–97.
21. Kurokawa T, Itagaki S, Yamaji T, *et al.* Antioxidant Activity of a Novel Extract from Bamboo Grass (AHSS) against Ischemia-Reperfusion Injury in Rat Small Intestine. *Biol Pharm Bull* 2006;29:2301–3.
22. Vardi N, Parlakpınar H, Ozturk F, *et al.* Potent protective effect of apricot and β -carotene on methotrexate-induced intestinal oxidative damage in rats. *Food Chem Toxicol* 2008;46:3015–22.
23. Winterbourn C, Hawkins R, Brian M, Carrell R. The estimation of red cell superoxide dismutase activity. *J Lab Clin Med* 1975;85:337–41.
24. Guneli E, Cavdar Z, Islekel H, *et al.* Erythropoietin protects the intestine against ischemia/ reperfusion injury in rats. *Mol Med* 2007;13:509–17.
25. Gamble M. The Hematoxylin and Eosin. In: Bancroft, JD and Gamble M, editor. *Theory and Practice of Histological Techniques*. 6th ed. Philadelphia: Churchill Livingstone Elsevier; 2008:121–34.
26. Jones ML, Bancroft JD, Gamble M. Connective Tissues and Stains. In: Bancroft, JD and Gamble M, editor. *Theory and Practice of Histological Techniques*. 6th ed. Philadelphia: Churchill Livingstone Elsevier; 2008:135–60.
27. Buchwalow IB, Böcker W. Working with Antibodies. In: *Immunohistochemistry: Basics and Methods*. Springer Berlin Heidelberg; 2010:31–9.
28. Ibrahim MAA, Elbakry RH, Bayomy NA. Effect of bisphenol A on morphology, apoptosis and proliferation in the resting mammary gland of the adult albino rat. *Int J Exp Pathol* 2016;97:27–36.
29. Dawson B, Trapp RG. Basic & Clinical Biostatistics. In: *Basic & Clinical Biostatistics*. 4th ed. Lange Medical Books / McGraw-Hill Medical Publishing Division; 2004:162–89.
30. Grippo AJ, Francis J, Beltz TG, Felder RB, Johnson AK. Neuroendocrine and cytokine profile of chronic mild stress-induced anhedonia. *Physiol Behav* 2005;84:697–706.
31. Ryu K-Y, Roh J. The Effects of High Peripubertal Caffeine Exposure on the Adrenal Gland in Immature Male and Female Rats. *Nutrients* 2019;11:951.
32. Gannouni N, Mhamdi A, El May M, Rhouma K, Tebourbi O. Morphological changes of adrenal gland and heart tissue after varying duration of noise exposure in adult rat. *Noise Heal* 2014;16:416.
33. Filho CB, Jesse CR, Donato F, *et al.* Chronic unpredictable mild stress decreases BDNF and NGF levels and Na⁺,K⁺-ATPase activity in the hippocampus and prefrontal cortex of mice: Antidepressant effect of chrysin. *Neuroscience* 2015;289:367–80.
34. Boyle MH, Paranjpe MG, Creasy DM. High Background Incidence of Spontaneous Subcapsular Adrenal Gland Hyperplasia of Tg.rasH2 Mice Used in 26-week Carcinogenicity Studies. *Toxicol Pathol* 2018;46:444–8.
35. Patra S, Rath S, Dutta BK, *et al.* Histological Study of Adrenal Gland In Case Of Suicidal Deaths. *IOSR J Dent Med Sci* 2014;13:30–6.

36. Wei L, Li Y, Tang W, *et al.* Chronic Unpredictable Mild Stress in Rats Induces Colonic Inflammation. *Front Physiol* 2019;10:1228.
37. Zhong J, Li G, Xu H, Wang Y, Shi M. Baicalin ameliorates chronic mild stress-induced depression-like behaviors in mice and attenuates inflammatory cytokines and oxidative stress. *Brazilian J Med Biol Res = Rev Bras Pesqui medicas e Biol* 2019;52:e8434–e8434.
38. Demirtaş T, Utkan T, Karson A, Yazır Y, Bayramgürler D, Gacar N. The Link Between Unpredictable Chronic Mild Stress Model for Depression and Vascular Inflammation? *Inflammation* 2014;37:1432–8.
39. Radwan D, El-Helbawy N, Salem M, El-Sawaf M. Effect of monosodium glutamate on body weight and the histological structure of the zona fasciculata of the adrenal cortex in young male albino rats. *Tanta Med J* 2017;45:104.
40. Bologna-Molina R, Mosqueda-Taylor A, Molina-Frechero N, Mori-Estevez A-D, Sánchez-Acuña G. Comparison of the value of PCNA and Ki-67 as markers of cell proliferation in ameloblastic tumors. *Med Oral Patol Oral Cir Bucal* 2013;18:e174–9.
41. Bozzo AA, Soñez CA, Monedero Cobeta I, *et al.* Chronic Stress Effects on Adrenal Cortex Cellular Proliferation in Pregnant Rats. *Int J Morphol* 2011;29:1148–57.
42. Finco I, Mohan DR, Hammer GD, Lerario AM. Regulation of stem and progenitor cells in the adrenal cortex. *Curr Opin Endocr Metab Res* 2019;8:66–71.
43. Steenblock C, Celis MFR de, Silva LFD, *et al.* Isolation and characterization of adrenocortical progenitors involved in the adaptation to stress. *Proc Natl Acad Sci* 2018;115:12997–3002.
44. Almeida H, Ferreira J, Neves D. Macrophages of the adrenal cortex: a morphological study of the effects of aging and dexamethasone administration. *Ann N Y Acad Sci* 2004;1019:135–40.
45. Fulda S, Gorman AM, Hori O, Samali A. Cellular stress responses: cell survival and cell death. *Int J Cell Biol* 2010;2010:214074.
46. Takhshid MA, Mehrabani D, Ai J, Zarepoor M. The healing effect of licorice extract in acetic acid-induced ulcerative colitis in rat model. *Comp Clin Path* 2011;21:1139–44.
47. Mohamed NE-S. Effect of Aqueous Extract of *Glycyrrhiza glabra* on the Biochemical Changes Induced by Cadmium Chloride in Rats. *Biol Trace Elem Res* 2018;190:87–94.
48. Rashwan NM, Anfenan MLK. Free radical scavenger effects of licorice on the experimental rats. *J appl sci res* 2012;8:4704–10.
49. Dogan SC, Baylan M, Erdoğan Z, Küçükgül A, Bulancak A. The Effects of Licorice (*Glycyrrhiza glabra*) Root on Performance, Some Serum Parameters and Antioxidant Capacity of Laying Hens. *Brazilian J Poultry Sci* 2018;20:699–706.
50. Ghorashi M, Rezaee MA, Rezaie MJ, Mohammadi M, Jalili A, Rahmani MR. The attenuating effect of aqueous extract of licorice on bleomycin-induced pulmonary fibrosis in mice. *Food Agric Immunol* 2017;28:67–77.
51. Cherng J-M, Lin H-J, Hung M-S, Lin Y-R, Chan M-H, Lin J-C. Inhibition of nuclear factor κ B is associated with neuroprotective effects of glycyrrhizic acid on glutamate-induced excitotoxicity in primary neurons. *Eur J Pharmacol* 2006;547:10–21.
52. Bode AM, Dong Z. Chemopreventive Effects of Licorice and Its Components. *Curr Pharmacol reports* 2015;1:60–71.
53. Fukuchi K, Okudaira N, Adachi K, *et al.* Antiviral and Antitumor Activity of Licorice Root Extracts. *In Vivo (Brooklyn)* 2016;30:777–86.
54. Garg NK, Mangal S, Sahu T, Mehta A, Vyas SP, Tyagi RK. Evaluation of anti-apoptotic activity of different dietary antioxidants in renal cell carcinoma against hydrogen peroxide. *Asian Pac J Trop Biomed* 2011;1:57–63.
55. Zhou M, Liu L, Wang W, *et al.* Role of licochalcone C in cardioprotection against ischemia/reperfusion injury of isolated rat heart via antioxidant, anti-inflammatory, and anti-apoptotic activities. *Life Sci* 2015;132:27–33.
56. Fan Z-Z, Zhao W-H, Guo J, *et al.* [Antidepressant activities of flavonoids from *Glycyrrhiza uralensis* and its neurogenesis protective effect in rats]. *Yao Xue Xue Bao* 2012;47:1612–1617.
57. Aksoy N, Dogan Y, Iriadam M, *et al.* Protective and therapeutic effects of licorice in rats with acute tubular necrosis. *J Ren Nutr* 2012;22:336–43.

الملخص العربي

تأثير الإجهاد الخفيف المزمن غير المتوقع على قشرة الغدة الكظرية لدى الجرذان البالغة والدور الوقائي المحتمل لمستخلص العرقسوس: دراسة هستولوجية و هستوكيميائية مناعية

منى تيسير صادق، شيرين شوقي العبد، مروة عوض عبد الحميد إبراهيم

قسم الهستولوجيا وبيولوجيا الخلية - كلية الطب - جامعة طنطا

مقدمة: الإجهاد المزمن الذي يتصاعد بسبب أحداث الحياة المفاجئة والغير متوقعة هو عامل خطير لتطور الاكتئاب، ويمكن أن يثبط المناعة ويزيد من التعرض للأمراض الالتهابية. يستخدم مستخلص العرقسوس بكثرة في الطب التقليدي والحديث، خاصةً بسبب خصائصه المضادة للأكسدة والمضادة للالتهابات.

الهدف من العمل: يهدف هذا العمل إلى إجراء تقييم كيميائي حيوي و هستولوجي و هستوكيميائي مناعي لتأثير الإجهاد الخفيف المزمن غير المتوقع على بنية قشرة الغدة الكظرية للجرذان والدور التحسيني المحتمل لمستخلص العرقسوس المائي.

المواد وطرق البحث: تم تقسيم أربعة وعشرين من ذكور الجرذان البيضاء إلى ٤ مجموعات. الضابطة، المعالجة بالعرقسوس، مجموعة الإجهاد الخفيف المزمن غير المتوقع (تتعرض لضغوط متغيرة في نمط عشوائي غير متوقع لمدة ٤ أسابيع) مجموعة الإجهاد الخفيف المزمن غير المتوقع مع العرقسوس (مثل المجموعة الثالثة بالإضافة إلى ٣٠٠ مجم/كجم/يوم من خلاصة العرقسوس). تم قياس الألدوستيرون والكورتيكوستيرون في البلازما. تمت معالجة عينات قشرة الغدة الكظرية لإجراء دراسة كيميائية حيوية و هستولوجية و هستوكيميائية مناعية.

النتائج: أظهرت مجموعة الإجهاد الخفيف المزمن غير المتوقع زيادة ذات دلالة إحصائية في الألدوستيرون والكورتيكوستيرون والمالونديالدهيد والميلوبيروكسيداز النسيجي مع انخفاض ذي دلالة إحصائية في الجلوتاثيون وأكسيد السوبر ديسميوتاز النسيجي. كشف الفحص الهستولوجي عن زيادة في سماكة الغشاء الكظري وتضخمه، واضطراب في النمط التكويني المنتظم وسماكة جميع المناطق وتغيرات خلوية في شكل تشوهات نووية وفجوات في السيتوبلازم. تم تسجيل زيادة ذات دلالة إحصائية في كل من التعبير الهستوكيميائي المناعي ل-caspase-٣ و PCNA بينما أوضحت المجموعة التي تمت معالجتها بشكل مشترك مع العرقسوس قيم شبه طبيعية لمعظم الدلالات مع شكل هستولوجي شبه طبيعي لقشرة الغدة الكظرية.

الاستنتاج: يمكن أن يكون العرقسوس مفيداً في السيطرة على الآثار الضارة التي يسببها الإجهاد الخفيف المزمن غير المتوقع على حالة الأكسدة و شكل قشرة الغدة الكظرية و موت الخلايا المبرمج و تكاثرها فيها على الأرجح من خلال خصائصها المضادة للأكسدة والمضادة للالتهابات ومضادة للتكاثر.